Received: April 28, 2022. Revised: July 13, 2022.

INASS

International Journal of
Intelligent Engineering & Systems

http://www.inass.org/

Inverter Control on 3 Phase UPS System as Harmonic Compensator and Power Factor Improvement Using Online Combined Error Adaptive Fuzzy

Dedy Kurnia Setiawan[1]* **Widya Cahyadi[1]** **Bambang Sri Kaloko[1]**

[1]*Department of Electrical Engineering, Universitas Jember, Jember 68121, Indonesia*
* Corresponding author's Email: dedy.kurnia@unej.ac.id

Abstract: Uninterruptible power supply (UPS) is a form of electrical supply that is frequently used to regulate electrical current and perform as a backup power source when the primary power source fails. Apart from providing backup power, the inverter system proposed in this study can reduce harmonic effects and increase power factor. The control system is based on a synchronized reference frame (SRF) and uses online combined error adaptive fuzzy (OCEAF). The load voltage and current are decomposed into their symmetrical components: positive, negative, and zero. These components are then transformed to a synchronous reference frame (dq), which OCEAF controls. Controlling the inverter is accomplished by converting the controller output to abc coordinates. OCEAF combines the delta error adaptive fuzzy (DEAF) and the absolute error adaptive fuzzy (AEAF) techniques with the NN adaptor. This adaptive fuzzy-PI automatically modifies the *Kp* and *Ki* values when the system changes, significantly when the source value alters or is faulty. According to power factor measurements, OCEAF performance is superior, more consistent, and closely unity power factor. As for evaluating network harmonics, systems with OCEAF controllers may reduce network harmonics from 6.24 % to between 1 and 1.5 %. The DEAF and CEAF techniques reduce harmonics by 2-2.5 and 1.5-2 %, respectively.

Keywords: Three-phase AC/DC converter, Uninterruptible power supply, Combined error adaptive fuzzy, Delta error adaptive fuzzy.

1. Introduction

Electrical energy demand has increased due to technological advancements for both residential and industrial customers. Numerous load types, both linear and nonlinear, have advanced fast. This increase has a noticeable effect on the electrical system's functioning. The formation of harmonics is one of the undesirable consequences of the presence of nonlinear loads. Not only do harmonic-distorted currents have a fundamental frequency of 50 Hz, but they also have multiple high-frequency components. When harmonic current interacts with the impedance of the mains power supply, line voltage distortion results, and harmonics in the electrical system can result in line and transformer losses. Eddy's current losses are one of them. These losses occur in the iron core due to the coil's induced current flowing through it. This current has the potential to overheat the transformer. The component of these losses is proportional to the square of the frequency of the induced current [1–6]. Additionally, unbalanced inductive or capacitive loads can change the power factor or cos θ. A poor power factor pulls a larger internal current, and the resulting excessive heat damages or shortens the life of the equipment. Furthermore, increased reactive loads might decrease the output voltage, causing damage to sensitive equipment.

Active filters are one of the numerous techniques attempted to resolve this issue. There are also other further choices. Active filters can improve the overall quality of the electric power provided by an electrical system, particularly on the source side or distribution network. Depending on the selected control mechanism, the duty of compensating for the active filter can be accomplished in various ways. An active filter circuit is a specific type of inverter controlled

by a particular control technique, albeit it is an inverter in general.

On the other hand, as customer needs for electrical energy continuity increase, the use of the uninterruptible power system (UPS) expands. Numerous electrical gadgets are fitted with UPSs as a kind of interference protection. A UPS system converts a DC supply to three-phase AC through an inverter like an active filter. Thus, the UPS may also operate as an active filter with proper supervision, compensating for harmonics and correcting the power factor. UPS is one among them. Online UPSs can minimize harmonics and enhance power factors solely on the protected load side [7–9].

A modified synchronous reference frame (MSRF) control approach was used in another investigation [10–13]. These approaches are based on the breakdown of primary source three-phase voltages and currents into their symmetrical sequence components, namely positive, negative, and zero voltages are translated into *dq* coordinates [14]. As a result, the voltage and current magnitudes may be regulated concerning the reference DC signal. PI is used to control the amount of current and voltage utilized. The controller's shortcoming is the tuning system's inability to obtain the proper proportional constant (*Kp*) and integral constant (*Ki*). This is exacerbated if the system undergoes considerable modifications, as tuning will be required each time a change happens.

This work proposes a control mechanism for accurately and automatically tuning the Kp and Ki parameters to enhance the aforementioned circumstances. Self-tuning fuzzy-PI is used as the controller approach. This logic control provides several benefits over programmable logic controllers. One of them is that it is not dependent on a mathematical model and can function more effectively with nonlinear systems [14, 15].

Numerous research has demonstrated that an adaptive fuzzy controller may be employed to regulate the inverter. To derive the constants *Kp* and *Ki*, this approach typically employs an error signal (e) and a delta error signal (de) as input signals. The adaptive controllers used in this work were dubbed delta error adaptive fuzzy (DEAF) and absolute error adaptive fuzzy (AEAF). Both of these control mechanisms use identical input, except that the error value in AEAF is an absolute value [16–18].

In the previous study, a mixture of DEAF and CEAF was used. Each adaptive fuzzy is accountable for independently determining Kp and Ki values [16]. In this field, it is state of the art. Compared to the DEAF and AEAF approaches, this system's response is more precise. When applied to UPS, however, this CEAF approach still has flaws. It has a slower response time and steadier steady-state stability with more ripples. To improve this controller, CEAF adjustments were required. Before CEAF, an online artificially intelligent adaptor must be introduced to condition the control signal. In this study, a neural network (NN) controller was utilized. Online combined error adaptive fuzzy (OCEAF) describes the combination of the CEAF controller with the NN adaptor.

The OCEAF approach is a novel adaptive fuzzy technique applied in this study. OCEAF combines DEAF and AEAF in a fuzzy and neural network manner. In this study, the neural network architecture is employed to execute fuzzy logic inference, with the a priori knowledge of each rule directly encoded into the network weights. When the input is a sharp set, the suggested neural network architecture's functionality is reduced to sharp *mode ponens*. Each adaptive fuzzy is responsible for individually establishing the values of *Kp* and *Ki*.

This research aims to determine the performance of an inverter coupled to an OCEAF controller that functions as a UPS and operates as a power factor and harmonics compensation. A UPS with a CEAF and a DEAF controller was used as a point of reference.

This essay is divided into several sections. The introduction, which discusses the context of the problem, is followed by the research technique section, which discusses the recommended strategy for resolving the problem. The following part, results and discussion, covers the simulation results testing and discussion and concludes with the conclusion section.

2. System description and modeling

The control approach depicted in Fig. 1 is based on the transformation of current and voltage to their symmetrical components. This control approach is referred to as a symmetrical sequence controller, and it comprises a three-channel layout comprising an inner current loop and an outside voltage loop. Three channels are utilized to regulate three distinct sequences.

DK Setiawan and colleagues [10, 13, 19] propose this technique based on a symmetrical sequence controller. The variables v^*_{dp}, v^*_{dn}, v^*_{dz}, v^*_{qp}, v^*_{qn}, and v^*_{qz} in this figure represent the reference voltages at coordinate dq. The voltage and current magnitudes obtained by transforming the abc coordinates' symmetry component to the dq coordinates are $v_{dq,p}$, $v_{dq,n}$, $v_{dq,z}$ and $i_{dq,p}$, $i_{dq\ n}$, $i_{dq,z}$.

In Fig. 1, the OCEAF controller block corresponds to the OCEAF controller in Fig. 2. As

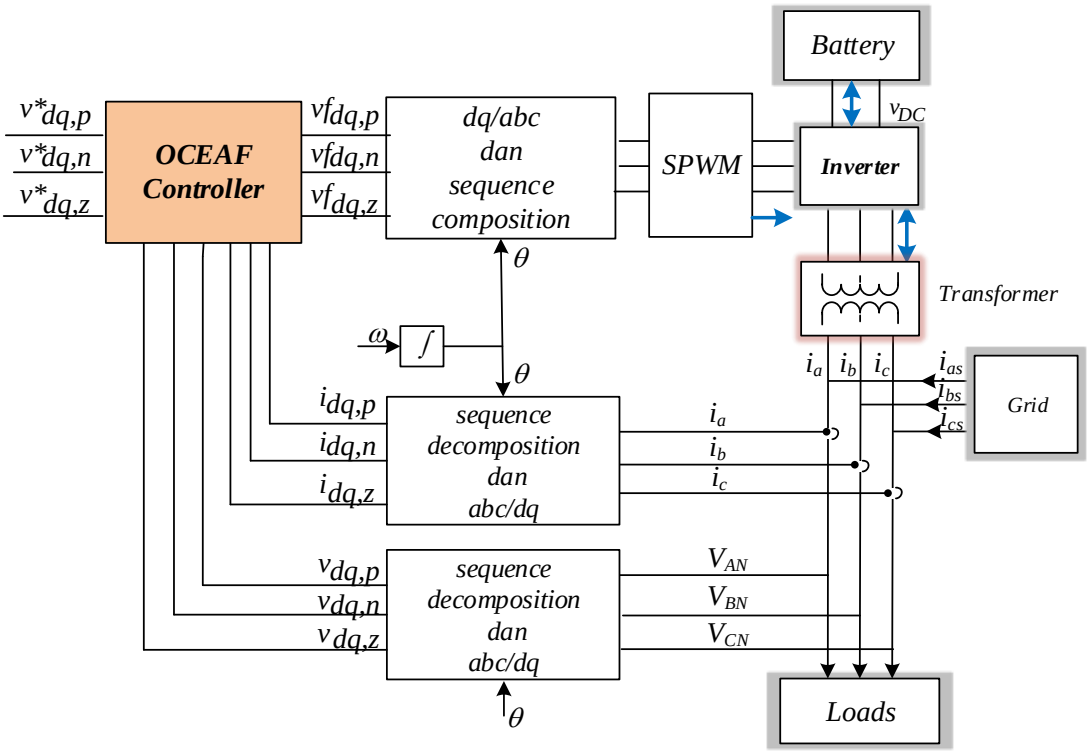

Figure. 1 OCEAF-based inverter control model for a UPS

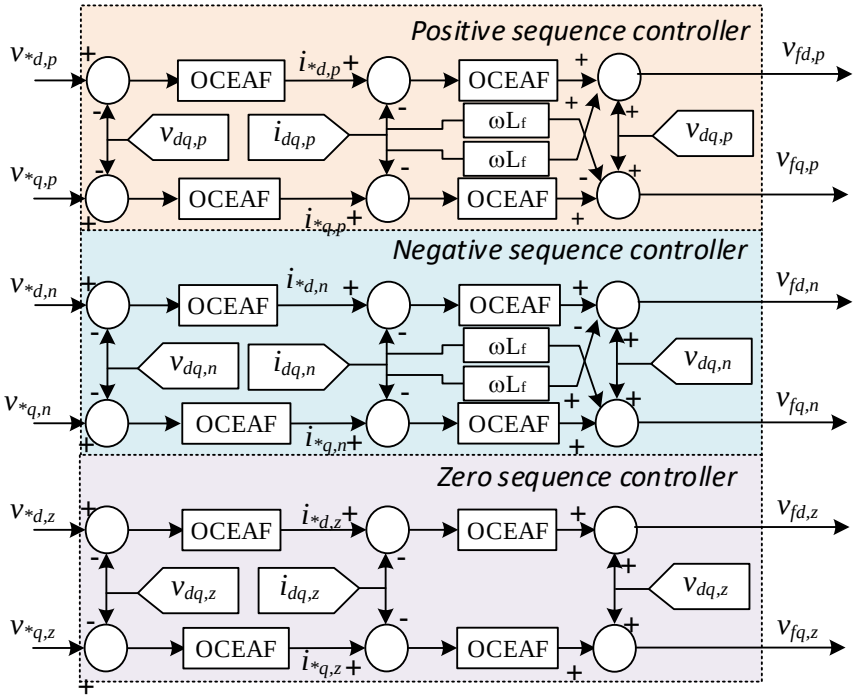

Figure. 2 Schematic representation of the OCEAF controller

can be seen from these two pictures, this inverter is controlled by two loops. The outer loop is a variable voltage controller, whereas the inner loop is a variable current controller.

2.1 Sequence decomposition and abc/dq transformation

In harmonic interference, the voltage and current waves are mismatched. This wave is divided into three equal phasors using the symmetrical sequence components [20].

Received: April 28, 2022. Revised: July 13, 2022.

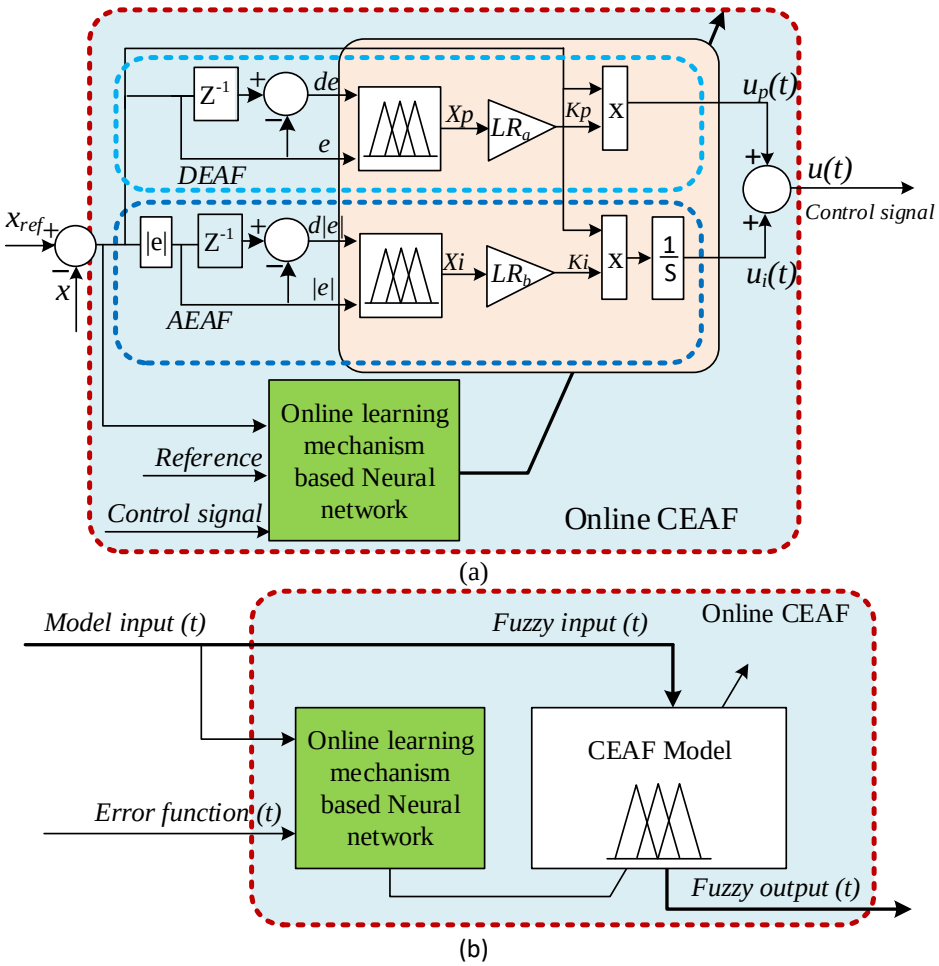

Figure. 3 The UPS control system uses the proposed OCEAF: (a) The OCEAF PI controller's structure and (b) OCEAF model diagram

The clark and park transformation turns the voltage and current obtained from the decomposition of the preceding equation into *dq* coordinates at the fundamental frequency.

The variable *y* denotes the voltage or current, X_1(t) denotes the fundamental input signal, and X_2(t) denotes the fundamental input signal shifted by 90 degrees.

$$y_p(t) = \frac{1}{3}\begin{bmatrix} 1 & -0.5 & -0.5 \\ -0.5 & 1 & -0.5 \\ -0.5 & -0.5 & 1 \end{bmatrix} X_1(t) - \frac{1}{2\sqrt{3}}\begin{bmatrix} 0 & 1 & -1 \\ -1 & 0 & 1 \\ 1 & -1 & 0 \end{bmatrix} X_2(t) \quad (1)$$

$$y_n(t) = \frac{1}{3}\begin{bmatrix} 1 & -0.5 & -0.5 \\ -0.5 & 1 & -0.5 \\ -0.5 & -0.5 & 1 \end{bmatrix} X_1(t) + \frac{1}{2\sqrt{3}}\begin{bmatrix} 0 & 1 & -1 \\ -1 & 0 & 1 \\ 1 & -1 & 0 \end{bmatrix} X_2(t) \quad (2)$$

$$y_z(t) = \frac{1}{3}\begin{bmatrix} 1 & 1 & 1 \\ -0.5 & -0.5 & -0.5 \\ -0.5 & -0.5 & -0.5 \end{bmatrix} X_1(t) + \frac{1}{2\sqrt{3}}\begin{bmatrix} 0 & 0 & 0 \\ -1 & -1 & -1 \\ 1 & 1 & 1 \end{bmatrix} X_2(t) \quad (3)$$

2.2 Outer voltage loop

The outer voltage loop is a control loop with voltage as the control variable. It is used to maintain a consistent voltage reading. This controller block has three controllers: a positive, a negative, and a homo polar or zero. Each controller independently controls the components of the positive, negative, and zero sequences.

The third-order voltage value is compared to the output reference voltage in this controller. The OCEAF controller processes the ensuing error. The peak voltage value for the positive sequence voltage reference is used, while the value for the negative and zero sequence voltage references is maintained constant. This loop generates reference currents

 DOI: 10.22266/ijies2022.1231.06

denoted by the symbols $i^*_{d,p}$, $i^*_{q,p}$, $i^*_{d,n}$, $i^*_{q,n}$, $i^*_{d,h}$, and $i^*_{q,h}$. The inner current loop uses these six variables as references.

2.3 Inner current loop

The output inner current loop generates SPWM's reference signal voltage. Based on Fig. 2, the reference signals for positive sequence($v_{fd,p}$ and $v_{fq,p}$), negative sequence ($v_{fd,n}$ and $v_{fq,n}$), and zero sequence ($v_{fd,z}$ and $v_{fq,z}$) are determined by (4) to (9). The OCEAF is shown in Fig. 3.

$$v_{fd,p} = v_{d,p} + (OCEAF)\left(i^*_{d,p} - i_{d,p}\right) + \omega L_f i_{q,p} \quad (4)$$

$$v_{fq,p} = v_{q,p} + (OCEAF)\left(i^*_{q,p} - i_{q,p}\right) - \omega L_f i_{d,p} \quad (5)$$

$$v_{fd,n} = v_{d,n} + (OCEAF)\left(i^*_{d,n} - i_{d,n}\right) - \omega L_f i_{q,n} \quad (6)$$

$$v_{fq,n} = v_{q,n} + (OCEAF)\left(i^*_{q,n} - i_{q,n}\right) + \omega L_f i_{d,n} \quad (7)$$

$$v_{fd,z} = v_{d,z} + (OECAF)\left(i^*_{d,z} - i_{d,z}\right) \quad (8)$$

$$v_{fq,z} = v_{q,z} + (OECAF)\left(i^*_{q,z} - i_{q,z}\right) \quad (9)$$

2.4 Transformation of dq/abc and sequence composition

A driver signal from SPWM is necessary for controlling the UPS. This signal results from inverting the translation of the control signal dq into abc coordinates. This modification employs the inverse clark and park transform in (10). With *x* represents voltage in positive sequence *p*, negative sequence *n*, or zero sequence *z*. The outcomes are then recompiled into the respective A, B, and C phase components (11).

$$\begin{bmatrix} v_{ax} \\ v_{bx} \\ v_{cx} \end{bmatrix} = \frac{2}{3}\begin{bmatrix} sin(\omega t) & cos(\omega t) \\ sin\left(\omega t - {}^{2\pi}/_{3}\right) & cos\left(\omega t - {}^{2\pi}/_{3}\right) \\ sin\left(\omega t + {}^{2\pi}/_{3}\right) & cos\left(\omega t + {}^{2\pi}/_{3}\right) \end{bmatrix}\begin{bmatrix} v_{dx} \\ v_{qx} \end{bmatrix} \quad (10)$$

$$\begin{bmatrix} v_a \\ v_b \\ v_c \end{bmatrix} = \begin{bmatrix} v_{ap}+v_{an}+v_{az} \\ v_{bp}+v_{bn}+v_{bz} \\ v_{cp}+v_{cn}+v_{cz} \end{bmatrix} \quad (11)$$

3. Control of inverters using online CEAF

This section describes the design of the system identifications that are used to compensate for the control signals generated by the previously mentioned current and voltage controllers. Fig. 3 illustrates the diagram for system modeling utilizing the online self-tuning fuzzy CEAF approach. Each of the system models has two inputs and a single output. The learning algorithm employs the gradient descent method and back-propagation with two inputs. It contributes to tuning the fuzzy input MF shapes and output weights to predict the model output accurately compared to the corresponding natural system.

The most often used self-tuning fuzzy control approach is the DEAF type controller. DEAF is a self-tuning fuzzy algorithm frequently used as a controller [7–11]. Generally, a proportional constant *Kp* or an integral constant *Ki* on a PI are determined using an error signal (*e*) and a delta error signal (*de*) as input signals.

Even when just one DEAF is employed, the DEAF fuzzy controller follows the same procedures for finding the values of *Kp* and *Ki*. Even though the personalities of *Kp* and *Ki* are unmistakably distinct. On the other hand, some additional adaptive fuzzy controllers are similar to DEAF but start with absolute error values and delta errors, which we refer to as AEAF in this work.

The OCEAF is employed in this research since it combines DEAF and AEAF. Fig. 3 illustrates this control approach. Each adaptive fuzzy controller controls the *Kp* and *Ki* values independently. As a result, it is projected to provide more accurate and reliable performance than the prior technique.

The value of *Kp* is computed using DEAF with up to two variables as inputs. The first parameter is an error, denoted by e(t); the difference between a reference value and a measured value, such as the magnitude of a voltage or current. Eq. (11)'s DC voltage error is a fuzzy input to the voltage controller. Two DEAF inputs are often utilized with current controllers and input error variables (e) currents i_d and i_q. Eqs. (12) and (13) demonstrate this.

$$e_1(k) = v_{dc,ref} - v_{dc}(k) \quad (11)$$

$$e_2(k) = i_{d,ref} - i_d(k) \quad (12)$$

$$e_3(k) = i_{q,ref} - i_q(k) \quad (13)$$

where k denotes the discrete-time interval, i_d and i_q denote the real currents, and $i_{d,ref}$ and $i_{q,ref}$ denote the reference flows in the frame dq,.

The DEAF controller's second input is the delta error (de), which is calculated as the difference between the error and the prior input error, as seen in Eqs. (14) and (15).

$$de_2(k) = e_2(k) - e_2(k-1) \quad (14)$$

$$de_3(k) = e_3(k) - e_3(k-1) \quad (15)$$

The DEAF fuzzy membership function (MF) is as follows for each input and output: The MFs for *e*(*k*) and *de*(*k*) is defined using the type "trimf" in five functions. The triangular MF compares high-variance changes in current or voltage values. The benefit is that it can detect minute changes in current or voltage and recommend quick and precise control options for the inverter control process.

As seen in Fig. 4, the MFs employed are negative large (NL), negative small (NS), zero (Z), positive small (PS), and positive large (PL). In terms of the output value *Kp*(k), the five MFs are as follows: zero (Z), positive small (PS), positive medium (PM), positive large (PL), and positive very large (PVL). These MFs are seen in Fig. 5. The current and voltage controllers' rule basis is created and shown in Table 1 for *Kp*.

The adaptive fuzzy AEAF controller is used to determine the value of *Ki*. Absolute error and absolute delta error are used as input variables. The absolute error of voltage or current controllers is the difference between the reference voltage or current and the rated voltage or current.

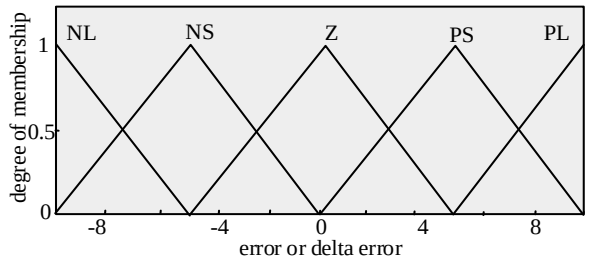

Figure. 4 MFs for DEAF input: e and de

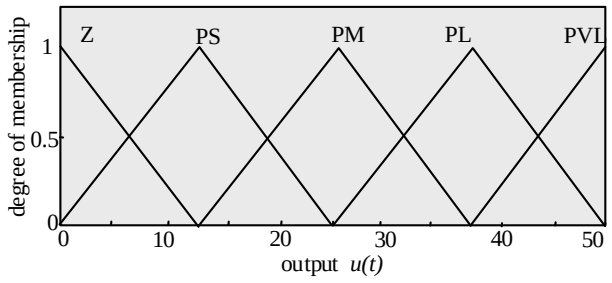

Figure. 5 MFs for output DEAF: *Kp*

Table 1. The basis of the *Kp* rule on DEAF

e	*de*				
	NL	NS	Z	PL	PL
NL	PVL	PL	PM	PS	Z
NS	PL	PM	PS	Z	PS
Z	PM	PS	Z	PS	PVL
PS	PS	Z	PS	PVL	PL
PL	Z	PS	PVL	PL	PM

Table 2. The basis of the *Ki* rule on AEAF

e	*de*				
	Z	VS	S	L	VL
Z	Z	Z	Z	VS	VS
VS	VS	VS	VS	S	S
S	S	S	S	L	L
L	L	L	L	L	VL
VL	VL	VL	VL	VL	VL

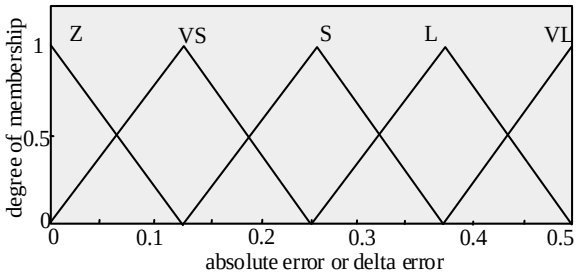

Figure. 6 MFs for AEAF input: |*e*| dan d|*e*|

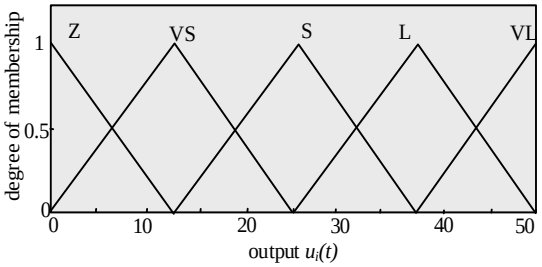

Figure. 7 MFs for output AEAF: *Ki*

As seen in Figs. 6 and 7, the set of AEAF MFs for input and output is specified as zero (Z), very small (VS), small (S), large (L), and very large (VL). The AEAF fuzzy rule matrix in Table 2 is based on the dynamic behavior of the error signal.

Because all of the MFs (μ^M) are triangular forms, they may be expressed as (16).

$$\mu^M(\mu^M) = 1 - \frac{2\left|x^M - a_j^M\right|}{b_j^M}, \quad j = 1,2 \ldots. \quad (16)$$

where x^M denotes the model input in its entirety, a_j^M denotes the center of the j^{th} triangle MF, and b_i^M denotes its width. We can compute the fuzzy output for the recognized fuzzy model's input as (17).

$$u^M = \frac{\sum_{j=1}^{k} \mu_j^M w_j^M}{\sum_{j=1}^{k} \mu_j^M} \quad (17)$$

where μ_j and w_j denote the height and weight, respectively, of the control output produced from the rule j^{th}. The model output y^M (Fig. 7) may be calculated as (18) from the fuzzy output:

$$y^M = \frac{1}{1+e^{-u^M}} \quad (18)$$

The neural-fuzzy recognized model's output y^M contains single output functions: *Kp* or *Ki*. Meanwhile, the model error function is defined as (19).

$$E = \frac{1}{2}\left(y^M(t) - y_{ref}^M\right)^2 \quad (19)$$

3.1 Three phase main source and battery

Assume that a three-phase alternating current source provides the electrical system with a specified power capacity of 5 MVA, an impedance Z = 6.75 % with X/R = 12.14, a voltage $V_{L\text{-}N}$ = 220 volts, a voltage $V_{L\text{-}L}(rms)$ = 380 volts, and a frequency, f = 50 Hz. According to these values, the impedance of the three-phase primary source is composed of a resistance R_s = 15.926 mΩ and an inductance L_s = 0.615 mH.

The battery is programmed to maintain its rated voltage and capacity. The battery block comprises of a direct current source with a voltage of 600 volts connected in parallel with a capacitor serving as a temporary storage device.

3.2 Load parameters

a. Resistive load

When the OCEAF inverter is tested as a UPS, a resistive load is employed with the phase values balanced. The load is 10 kΩ in each phase with a star connection (wye) as indicated in Fig. 8, for a total power of 10,000 Watts.

b. Low-power-factor loads

RL loads are used to evaluate the success of OCEAF management while attempting to enhance the power factor. This power factor improvement testing system utilizes an imbalanced RL load. This is since each phase will have a unique power factor value.

Fig. 9 illustrates the value of an unbalanced circuit with a low power factor. Additionally, Table 3 illustrates the power factor for each load phase, causing the network's current to lag (lagging behind the voltage).

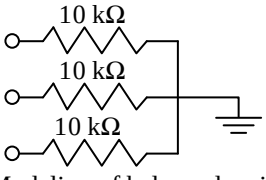

Figure. 8 Modeling of balanced resistive loads

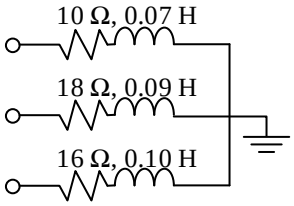

Figure. 9 Modeling of low power factor loads

Table 3. Loads with a low power factor for each phase

Phase	Loads		Power factor
	R (Ω)	L (H)	
A	10	0.07	0.41
B	18	0.09	0.53
C	16	0.1	0.454

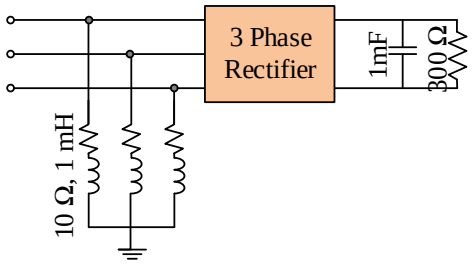

Figure. 10 Modeling of a nonlinear load

Table 4. System specification

No	Parameters		Value
1	Input and output Inverter	Battery input voltage	700 V
		Output voltage (V_{LN})	220 V
		Frequency	50 Hz
2	Filter	Inductance (L_f,)	0.3 mH
		Resistance (R_f)	0.1
3	Input and output main source	Output voltage (V_{AN})	220 V
		Frequency	50 Hz
		Rated power (3phase)	5 MVA

The load utilized as the test load in Fig. 9 has a low power factor value. As demonstrated in Table 3, the minimal power factor that may be accepted is roughly 0.87, but the load applied in this test is less than that. It will be demonstrated that by utilizing the OCEAF inverter control, the power factor may be improved to near unity.

c. Nonlinear load

A nonlinear load in the form of a three-phase rectifier is employed in the harmonic compensation test, as illustrated in Fig. 10. As seen in the figure, the load is a rectifier equipped with an input filter in the form of RL and a filter capacitor in parallel with a resistive load on the rectifier's output side. Under this load level, the network system will exhibit harmonic distortion.

4. Results and discussion

The proposed control approach was simulated using MATLAB. The parameters that were utilized are shown in Table 4. Before starting the OCEAF system, the 12 PI controllers in the control block lacked *Kp* and *Ki* values; however, the Kp and Ki values were automatically injected into the PI controllers once the system was started.

4.1 UPS Testing

During UPS testing, the grid voltage and current are intended to be deficient. As seen in Fig. 11, when a failure occurs at 0.075 seconds, the current is disconnected from its source. This disruption lasts from 0.125 and seconds. The system is enhanced by compensating for this circumstance with a fuzzy adaptive controller. The current situation following repair is depicted in Figs. 12(a) to 12(c). The system switches from its primary source to its backup supply during this mode, the UPS. Based on these three images, the controller employing OCEAF gives the most significant and most stable current response compared to other controllers.

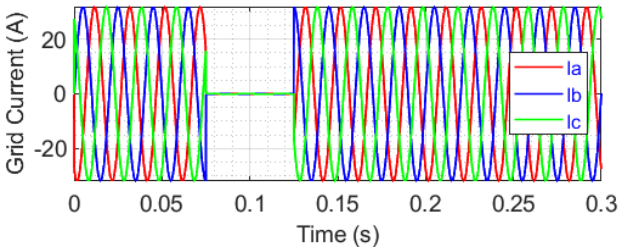

Figure. 11 Grid current (supply) when the fault occurs

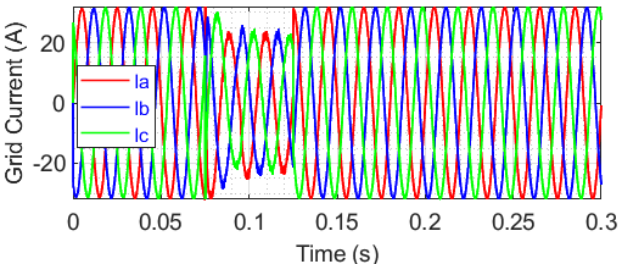

(a)

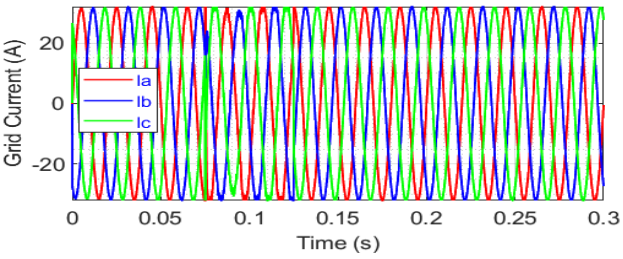

(b)

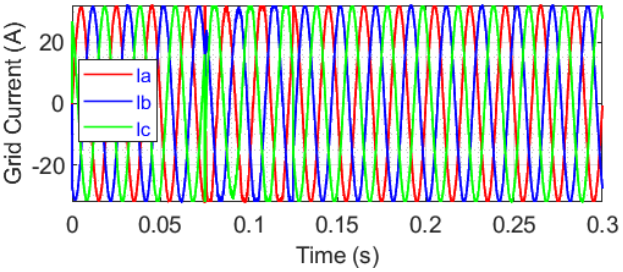

(c)

Figure. 12 Current system when UPS testing: (a) DEAF, (b) CEAF, and (c) OCEAF

When considered from the voltage perspective, the results will be as depicted in Fig. 13. When the

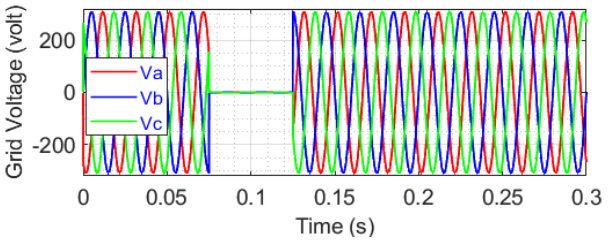

(a)

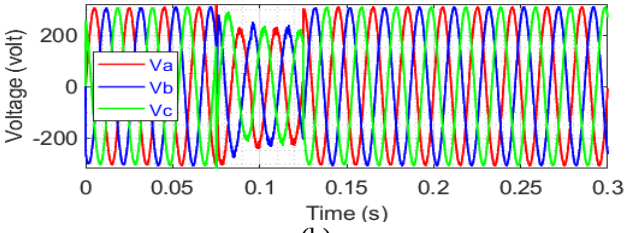

(b)

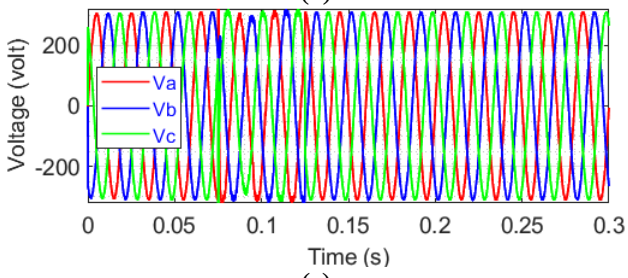

(c)

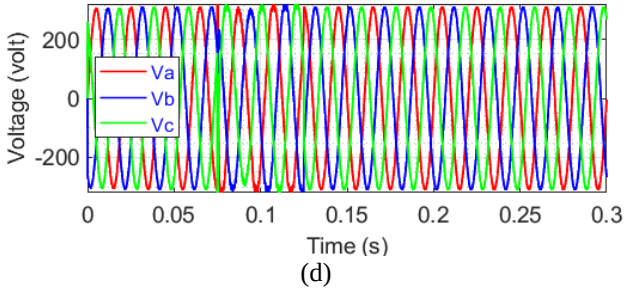

(d)

Figure. 13 Grid voltage system when UPS testing: (a) without compensator (b) DEAF, (c) OCEAF, and (d) OCEAF

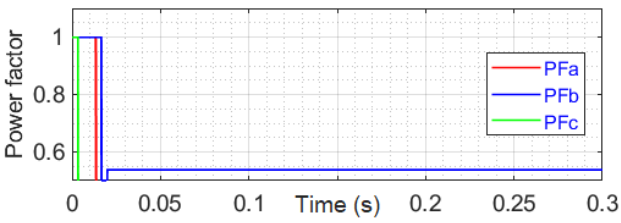

Figure. 14 Before system compensation, power factor graphs

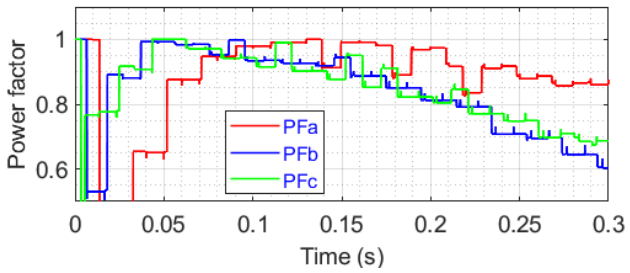

Figure. 15 Power factor system after compensation using DEAF

system has a foult, the voltage becomes 0 due to the interruption of grid current. By utilizing the OCEAF controller, the grid voltage can be maintained at a more stable level. Compared to the output voltages of other controllers, it appears that the OCEAF controller generates a more stable current and voltage.

4.2 Power factor compensator

Before correcting the system, Fig. 14 shows the power factor values for each phase. Phases A, B, and C have power factors of 0.41; 0.53; and 0.454, respectively. In testing as a power factor compensator, an unbalanced load is utilized.

Each phase has its unique power factor. Before compensation, the power factor ranges between 0.41, 0.53, and 0.454 for phases A, B, and C when seen from the network side. After compensation, the OCEAF controller performs significantly better than the DEAF and CEAF controllers. On a DEAF controller, the power factor value varies from 0.6 to 1, but on a CEAF controller, it ranges from 0.8 to 1.

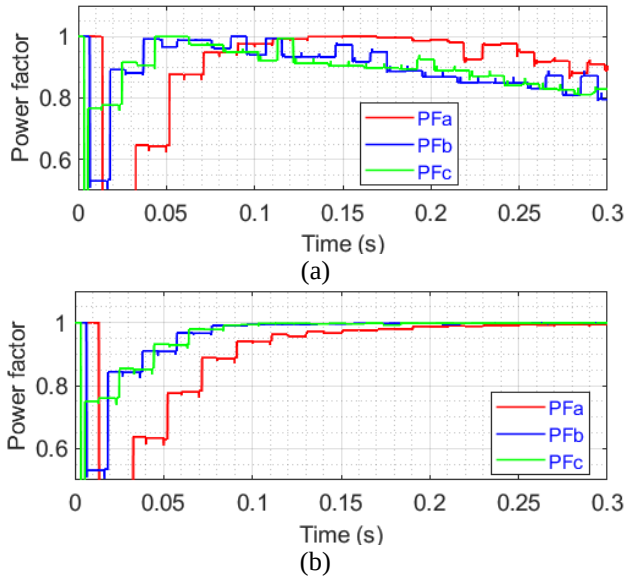

Figure. 16 Power factor system after compensation: (a)CEAF and (b) OCEAF

4.3 Harmonic current compensator

Harmonic distortion occurs in the current when the nonlinear load mentioned above is applied to the system. Fig. 17(a) shows that the output current is not a pure sine wave. Fig. 17(b) illustrates the present harmonic value. The resultant current appears to have a *THDi* value of 6.24 %, with the maximum value occurring in the fifth-order harmonic.

Using the suggested control method, the network

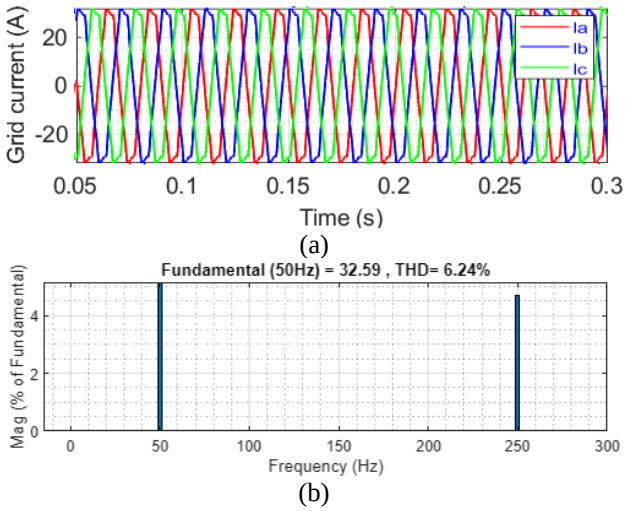

Figure. 17 Harmonic current testing before compensating: (a) grid current and (b) *THDi*

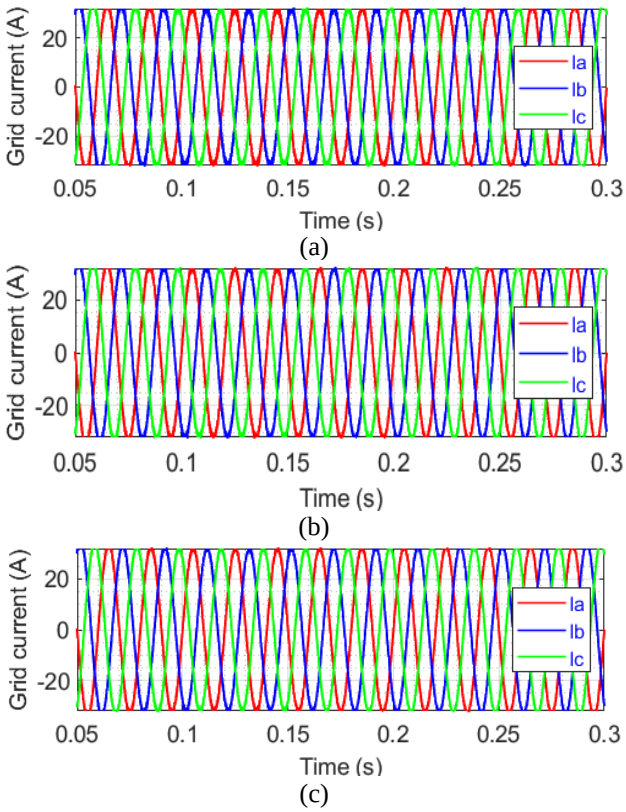

Figure. 18 Grid current after compensation: (a) DEAF, (b) DEAF, and (c) OCEAF

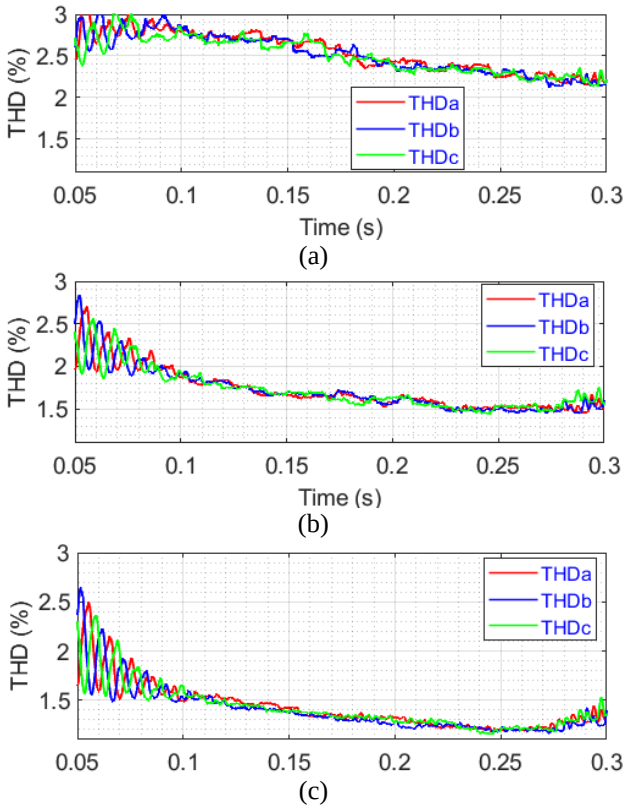

Figure. 19 The *THDi* current of network after compensation: (a) DEAF, (b) CEAF, and (d) OCEAF

current waveform improves and approaches a sinusoidal shape. Compared to the DEAF and CEAF controllers, the grid current with the OCEAF controller more closely resembles pure suns, as seen in Fig. 18. While the *THDi* value is displayed in Fig. 19, The *THDi* values of these controllers demonstrate that the OCEAF controller is superior.

The THDi's controller is between 1 and 1.5 % at steady-state, whereas it is 2-2.5 % for DEAF and 1.5-2 % for CEAF.

5. Conclusion

This article presents the OCEAF methodology as a self-tuning PI optimization method for the UPS. This controller allows this system to function as a power factor and harmonic compensator and be a UPS. The findings of 2.5 cycles of system testing as a UPS indicate that the OCEAF system performs better than DEAF and CEAF. In addition, based on power factor measurements, OCEAF performance is superior, more constant, and nearly unitary. As for harmonics testing, systems with OCEAF controllers can reduce network harmonics from 6.24 % to between 1 % and 1.5 %. The DEAF and CEAF methods reduce harmonics by 2-2.5 % and between 1.5 and 2 %, respectively.

Conflicts of interest

The authors declare that they have no conflict of interest.

Author contributions

Conceptualization, Dedy Kurnia Setiawan and Bambang Sri Kaloko; methodology, Dedy Kurnia Setiawan; software, Dedy Kurnia Setiawan and Widya Cahyadi; validation, Bambang Sri Kaloko; formal analysis and investigation, Dedy Kurnia Setiawan.

Notations

v^*dq, p	Voltage reference of positive sequence in dq coordinate
v^*dq, n	Voltage reference of negative sequence in dq coordinate
v^*dq, z	Voltage reference of zero sequence in dq coordinate
ω	Angular frequency = 2πf
L_f	Inductance
θ	Phase angle
THD_i	total harmonic distortion of current

References

[1] M. Sharifzadeh, H. Vahedi, A. Sheikholeslami, P. Labbé, and K. A. Haddad, "Hybrid SHM–SHE Modulation Technique for a Four-Leg NPC Inverter With DC Capacitor Self-Voltage Balancing", *IEEE Trans. Ind. Electron.*, Vol. 62, No. 8, pp. 4890–4899, 2015.

[2] D. K. Setiawan, M. Ashari, and H. Suryoatmojo, "Transient Operation of a Four-Leg Inverter in Rooftop Solar Connected to a Grid Using Optimized Constructive Neural Network", *Int. J. Intell. Eng. Syst.*, Vol. 14, No. 6, pp. 258–273, Dec. 2021, doi: 10.22266/ijies2021.1231.24.

[3] D. K. Setiawan, M. Ashari, and H. Suryoatmojo, "FLI for Unbalanced and Harmonic Current Mitigation in Rooftop Solar Connected Distribution Network", *Proc. - 2021 Int. Semin. Intell. Technol. Its Appl. Intell. Syst. New Norm. Era, ISITIA 2021*, pp. 173–178, Jul. 2021.

[4] Yongchang, Qin, Zhengxi, and Yingchao, "Comparative study of model predictive current control and voltage oriented control for PWM rectifiers", In: *Proc. of 2013 International Conference on Electrical Machines and Systems*

(ICEMS), pp. 2207–2212, 2013.

[5] A. Singh, “Multifunctional Capabilities of Grid Connected Distributed Generation System with Non-Linear Loads”, *Asian Journal of Control*, Vol. 18, pp. 1537– 1545, 2016.

[6] D. K. Setiawan, M. Ashari, and H. Suryoatmojo, "Harmonics Reduction for Four-Leg Distribution Network-Connected Single Phase Transformerless PV Inverter System Using Diagonal Recurrent Neural Network", In: *Proc. of 2019 International Conference of Artificial Intelligence and Information Technology*, pp. 331–335, 2019.

[7] Y. Ito and S. Kawauchi, "Microprocessor based robust digital control for UPS with three-phase PWM inverter", *IEEE Trans. Power Electron.*, Vol. 10, No. 2, pp. 196–204, 1995.

[8] D. K. Setiawan, Y. Megantara, and B. N. Syah, "Three phase inverter of UPS control system for harmonic compensator and power factor correction using modified synchronous reference frame", In: *Proc. of International Electronics Symposium* (*IES*), pp. 15-19, 2015, doi: 10.1109/ELECSYM.2015.7380806.

[9] K. H. Kim, N. J. Park, and D. S. Hyun, "Advanced Synchronous Reference Frame Controller for Three-phase UPS Powering Unbalanced and Nonlinear Loads", In: *Proc. of 2005 IEEE 36th Power Electronics Specialists Conference*, pp. 1699–1704, 2005.

[10] D.K Setiawan, M. Ashari, and M. H. Purnomo, "Diagonal recurrent neural network control of four-leg inverter for hybrid power system under fluctuating unbalanced loads", In: *Proc. of The Third International Student Conference on Advance Science and Technology* (*ICAST*), pp. 11-12. 2009.

[11] I. Vechiu, O. Curea, H. Camblong, S. Ceballos, and J. L. Villate, "Digital control of a three-phase four-leg inverter under unbalanced voltage conditions", In: *Proc. of 2007 European Conference on Power Electronics and Applications*, pp. 1–10, 2007.

[12] I. Vechiu, A. Etxeberria, and Q. Tabart, "Power quality improvement using an advanced control of a four-leg multilevel converter", In: *Proc. of 2015 IEEE 16th Workshop on Control and Modeling for Power Electronics (COMPEL)*, pp. 1–6, 2015.

[13] D. K. Setiawan, M. Ashari, and M. H. Purnomo, “Modified Synchronous Reference Frame untuk Pengendalian Inverter Empat Lengan pada Sistem Hibrida Generator Diesel dan Battery dengan Beban Tidak Seimbang”, *Journal Inf. Technol. Electr. Eng.*, Vol. 2, No. 1, 2010.

[14] I. Winarno, H. Suryoatmojo, and M. Ashari, "Hybrid PI-fuzzy controller based static var compensator for voltage regulation under uncertain load conditions", *J. Telecommun. Electron. Comput. Eng.*, Vol. 9, No. 2–5, 2017.

[15] S. Suwito, M. Ashari, M. Rivai, and M. A. Mustaghfirin, "Enhancement of Photovoltaic Pressurized Irrigation System Based on Hybrid Kalman Fuzzy", *Int. J. Intell. Eng. Syst.*, Vol. 15, No. 2, 2022, doi: 10.22266/ijies2022.0430.39.

[16] D. K. Setiawan, M. Ashari, H. Suryoatmojo, and W. Cahyadi, "Combined Error Adaptive Fuzzy–PI for Reducing DC Voltage Ripple in ThreePhase SPWM Boost Rectifier Under Unbalanced DGs System", *Int. J. Intell. Eng. Syst.*, Vol. 13, No. 3, pp. 384–395, 2020, doi: 10.22266/ijies2020.0630.35.

[17] C. Conker and M. K. Baltacioglu, "Fuzzy self-adaptive PID control technique for driving HHO dry cell systems", *International Journal of Hydrogen Energy*,Vol. 45, No. 49, pp 26059-26069, 2020.

[18]A. S. Wardhana, M. Ashari, and H. Suryoatmojo, "Optimal Control of Robotic Arm System to Improve Flux Distribution on Dual Parabola Dish Concentrator", *Int. J. Intell. Eng. Syst.*, Vol. 13, No. 1, pp. 364–378, 2020, doi: 10.22266/ijies2020.0229.34.

[19]Q. Tabart, I. Vechiu, A. Etxeberria, and S. Bacha, "Hybrid Energy Storage System Microgrids Integration for Power Quality Improvement Using Four-Leg Three-Level NPC Inverter and Second-Order Sliding Mode Control", *IEEE Trans. Ind. Electron.*, Vol. 65, No. 1, pp. 424–435, 2018.

[20] M. Ashari, D. K. Setiawan, and Soedibyo, "Inverter control for phase balancing of diesel generator — Battery hybrid power system using Diagonal Recurrent Neural Network", In: *Proc. of Australasian Universities Power Engineering Conference* (*AUPEC*), pp. 1-5, 2011.